Research Article

Research on the Temperature Field and Frost Heaving Law of Massive Freezing Engineering in Coastal Strata

Chaochao Zhang [,1,2] **Dongwei Li** [,1] **Junhao Chen** [,3] **Guanren Chen** [,1] **Chang Yuan** [,1] **Zecheng Wang** [,1] **Guosheng Ding** [,4] **Xin Chen** [,1] **Minghai Xia** [,5] **Shengfu Wang** [,1] **Bo Zhang** [,1] **Ru He** [,1] **and Xin Yi** [1]

[1]*School of Civil and Architecture Engineering, East China University of Technology, Nanchang 330013, China*
[2]*Nanjing Coal Mine Design & Research Institute, Nanjing 211800, China*
[3]*School of Civil Engineering, Fujian University of Technology, Fuzhou 350118, China*
[4]*Fuzhou Metro Co. Ltd., Fuzhou 350004, China*
[5]*Irrigation Management Office of Water Conservancy Project in Kuitun River Basin of Yili Kazak Autonomous Prefecture, Kuitun 833200, China*

Correspondence should be addressed to Dongwei Li; dwli2005@163.com

In this study, based on the background of massive freezing engineering in coastal strata, the thermal physical parameters and some freezing laws of soil were obtained through soil thermal physical tests and frozen soil frost heaving tests. When the freezing temperatures were −5°C, −10°C, −15°C, and −20°C, the frost heaving rates of the soil were 0.53%, 0.95%, 1.28%, and 1.41%, and the frost heaving forces of the soil were 0.37 MPa, 0.46 MPa, 0.59 MPa, and 0.74 MPa, respectively. In the range of test conditions, the frost heaving rate and the frost heaving force of the soil increased with the decrease of the freezing temperature, and the relationship was roughly linear with the temperature. The entire cooling process could be roughly divided into three stages: active freezing stage, attenuation cooling stage, and stability stage. The range of the frozen soil expansion did not increase linearly with the decrease of the freezing temperature, and there was a limit radius for the frozen soil expansion. A three-dimensional finite element model was established to simulate the temperature field and frost heaving of the soil under the on-site working conditions. The entire frost heaving process could be roughly divided into two stages. The calculated temperature values and the frost heaving force values were compared with the on-site measured values, and the results verified that the numerical calculation could accurately reflect the temperature field and frost heaving law of the formation.

1. Introduction

Natural frozen soil is mainly formed by the freezing of water in soil due to the low temperature of the natural environment. Artificial freezing is the use of artificial refrigeration to make the soil around the freezing pipe freeze. Then underground engineering construction is carried out under the protection of the freezing curtain. The artificial freezing method is an effective underground construction method that is widely used in mine construction and municipal engineering. Frozen soil is an extremely temperature-sensitive soil medium with rheological properties. Due to the

uneven distribution of moisture, soil can produce uneven frost heaving deformation, accompanied by the generation of a frost heaving force. Frost heaving can potentially cause many engineering problems, including road cracking, foundation damage, building tilt, freezing pipe fractures, tunnel collapse, and pipeline fractures. In natural permafrost areas, frost damage control is relatively passive, such as salt injection to treat subgrade frost damage. Artificial freezing is designed artificially, and its freezing range, temperature, and time are controllable. Therefore, compared with natural frozen soil, artificial freezing can better control the influence of frost heaving and thawing settlement on the original

environment and structures by controlling the freezing volume, rapid freezing, setting pressure relief holes, thawing settlement compensation grouting, and other measures.

Previous scholars have done a large amount of research on the theory of frozen soil frost heaving and the law of freezing and thawing, and they have achieved many results [1–5]. Wang et al. [6–9] studied the frost heaving characteristics and frost heaving force through frozen soil tests. Yue et al. [10] studied the variation laws of frozen soil temperature and frost heaving pressure. He et al. [11] put forward the coupling equations of water, heat, and force in the process of soil freezing. Xia et al. [12] and Wang et al. [13] analyzed the mechanical properties of frozen wall and studied the uneven frost heaving. Many achievements have been made regarding the theoretical derivation, field measurement, and numerical simulation of freezing temperature field [14–16]. Chen et al. [17–19] studied the law of the temperature field of frozen soil and its influencing factors based on a freezing project. Long et al. [20] carried out a model test and obtained the development law of the temperature. Zhang et al. [21] established a three-dimensional temperature field model and proposed a new frost heaving model. Li et al. [22] studied the optimal excavation time of soil and the variations of the saltwater temperature, soil temperature, surface performance, and tunnel deformation. Hu et al. [23–26] established a frozen soil finite element model to analyze the development law of the frozen temperature field.

In this study, based on massive freezing engineering in coastal strata, thermal physical tests and frost heaving tests were carried out to obtain the soil thermal physical parameters and the frost heaving law. Moreover, 3D numerical simulation was carried out to further explore the changes of the freezing temperature field and frost heaving law of the long connecting passage under the on-site freezing conditions. This study is expected to provide a reference for the design and construction of freezing projects.

2. Overview of Freezing Engineering and Soil Thermal Physical Parameters

2.1. Project Overview. In this study, a super long subway connecting passage was taken as the engineering background. The center distance of the connecting passage was 42.68 m, and the main body of the passage was located in silty soil and muddy sand. There were hot springs in the strata, resulting in a high ground temperature about 40°C. The connecting passage was reinforced by horizontal freezing and constructed with the mining method. The cross section of connecting passage and the freezing curtain is shown in Figure 1.

The excavation and the construction of the super long connecting passage took a long time, which led to the long freezing time for the freezing project. The connecting passage passed through a subway tunnel with a clear distance of about 7 m. Therefore, in the construction process of connecting passage, the accuracy of the frost heaving control was required to be high. If large frost heaving deformation were to occur, the building would be inclined

and cracked, the road or underground pipeline would be damaged, and the safety of the existing tunnel would be endangered, which would in turn cause a serious negative social impact.

2.2. Soil Thermal Physical Parameters. The main thermal physical parameters of each soil layer were obtained through experiments. The experimental results are shown in Table 1.

3. Frost Heaving Tests

3.1. Multifunctional Frost Heaving Testing Machine. The tests were carried out using a WDC-100 multifunctional frost heaving testing machine, which was composed of a loading system, a temperature control system, a moisture compensation system, and a measurement system. This machine could control the applied force, cold temperature, and ambient temperature. The test machine and the sample chamber are shown in Figures 2 and 3.

A cylindrical soil sample with dimensions $\varphi 50 \times 100$ mm is used, and the soil sample was placed in the sample chamber, as shown in Figure 3. There was a set of devices at the top and bottom of the soil sample. A refrigerant circulating pipe and a temperature sensor were arranged inside the device. The cold source was formed by circulating the refrigerant, and the temperature sensor monitored the temperature. A row of evenly distributed temperature measuring holes was set at the soil sample position of the sample cylinder. The distances between the temperature measuring holes and the bottom of the sample were 0.50 cm, 1.75 cm, 3.00 cm, 4.25 cm, 5.50 cm, and 6.75 cm. The temperature acquisition probes extended into the soil through the reserved temperature measuring hole to measure the relationship between the temperature inside the soil and the distance from the cold source.

3.2. Tests and Results Analysis. Single factor controlled frost heaving tests were carried out with the upper load being 0.6 MPa and the moisture content of the soil sample being 26%. The freezing temperatures adopted five levels of −5°C, −10°C, −15°C, −20°C, and −25°C, and the freezing time was 12 h. When considering the influence of the freeze-thaw cycles on the soil, the freezing temperature was −15°C, and the thawing temperature was 15°C. The designed freeze-thaw cycle was 24 h (12 h freezing and 12 h thawing) and the number of freeze-thaw cycles was six.

3.2.1. Temperature Field. The distribution of the soil temperature field for different cold source temperatures is shown in Figure 4, and the distribution of the soil temperature field for the freeze-thaw cycles is shown in Figure 5.

Figure 4 reveals the following:

(1) The entire cooling process could be roughly divided into three stages: the active freezing stage, the attenuation cooling stage, and the stability stage.

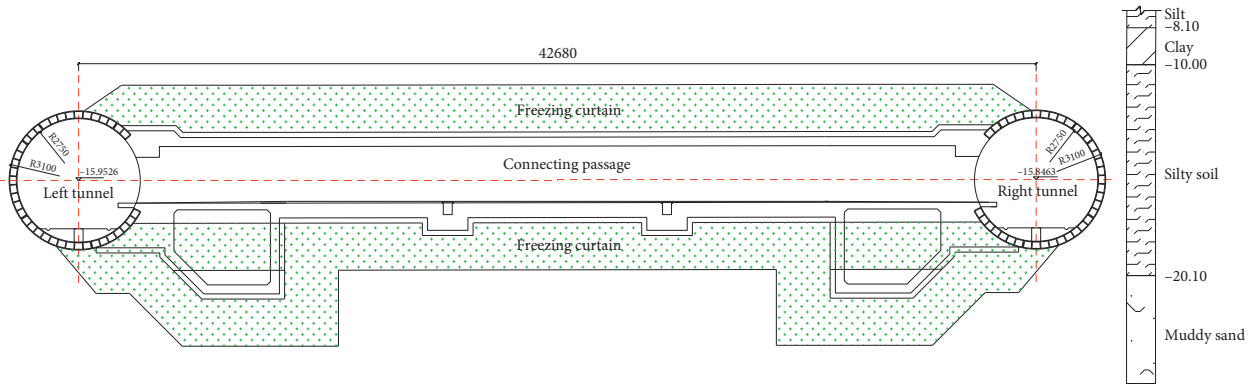(2) In the initial stage of freezing, the temperature of the soil was high and the temperature of the freezing

FIGURE 1: Cross section of connecting passage and freezing curtain.

TABLE 1: Thermal physical parameters of soil layer.

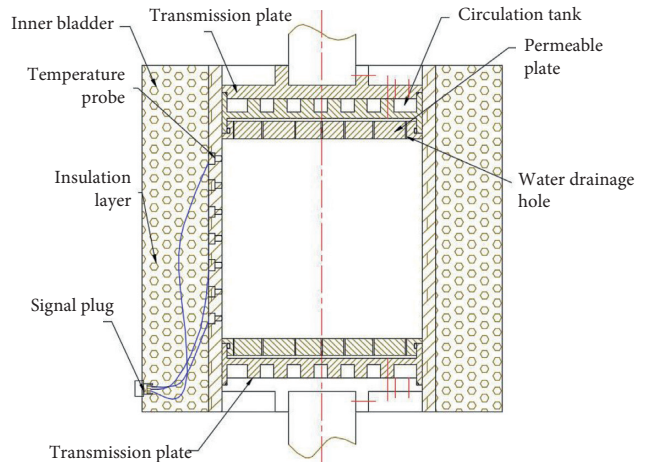| Layer	Soil properties	Moisture content (%)	Natural density (g·cm^{-3})	Thermal conductivity (w·m^{-1}°C^{-1})		Specific heat (J·kg^{-1}°C^{-1})	Freezing temperature (°C)
				13°C	−10°C		
1	Silt	55.38	1.98	1.327	1.423	1900	−2.3
2	Clay	24.79	2.13	1.470	1.651	1680	−1.5
3	Silty soil	44.04	2.04	1.286	1.731	1760	−1.8
4	Muddy sand	10.94	2.08	1.271	1.502	1520	−1.1

FIGURE 2: Appearance of the test machine.

FIGURE 3: Structure of sample chamber.

tube was very low. There was a large temperature difference between the freezing tube and the soil. The temperature gradient was large and the cooling rate of the soil was very fast. The active freezing stage was a stage in which the soil temperature dropped rapidly.

(3) With the decrease of the soil temperature, the temperature gradient between the freezing pipe and the soil decreased and the temperature rate of the soil decreased more. The water in the soil began to freeze and release latent heat, and the soil entered attenuation cooling stage.

(4) As the freezing time went by, the soil temperature continued to decrease. The temperature difference between the freezing pipe and the soil gradually decreased and the heat exchange generally tended to balance. The soil temperature dropped slowly and finally tended to be stable.

(5) The tendencies of the temperature changes at different measuring points were roughly the same. The closer the location was to the cold source, the faster the soil cooling rate was and the lower the stable temperature was. When the temperature of the cold source was −5°C, the final stable temperature of the farthest measuring point (6.75 cm away from the
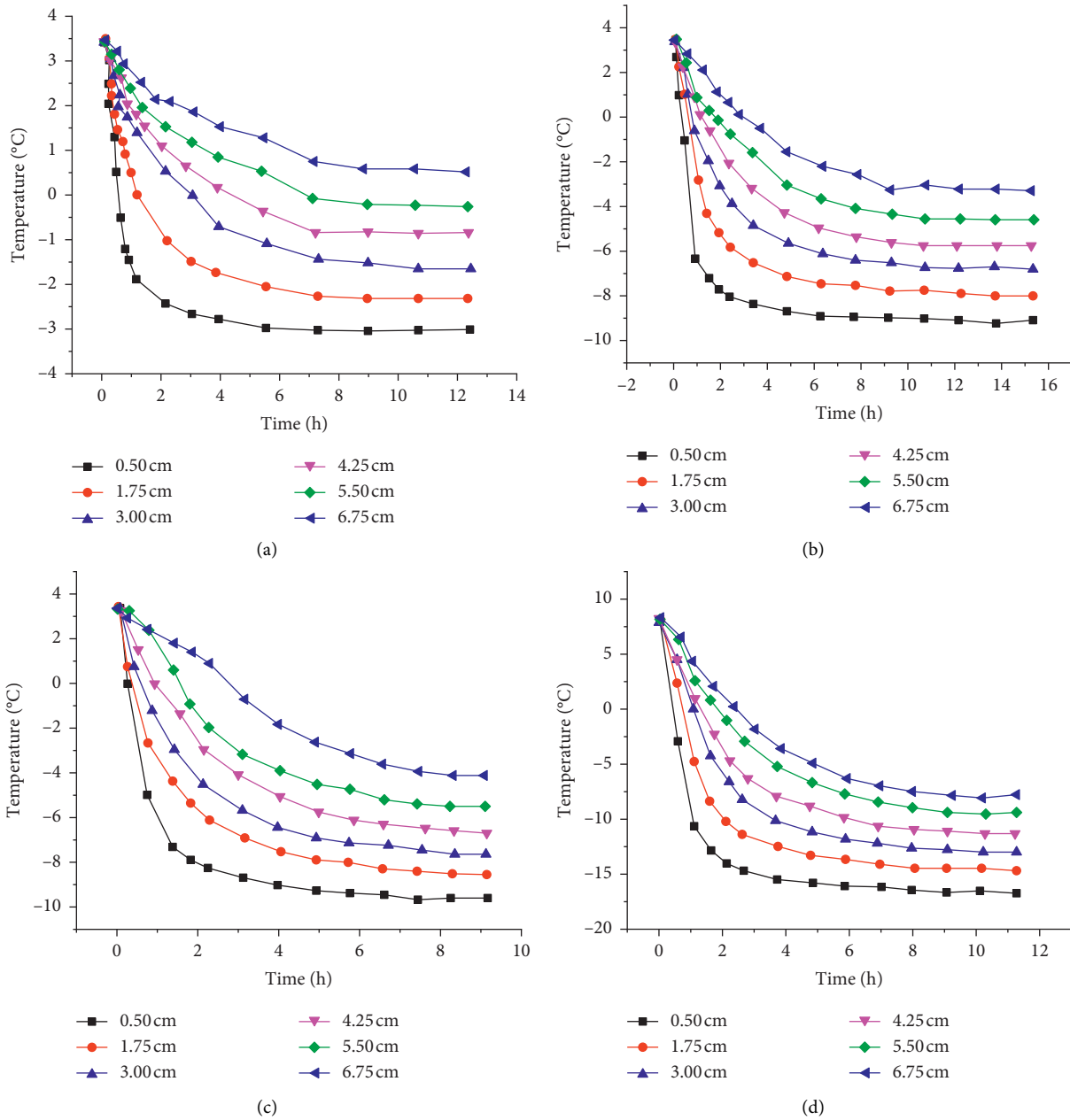
(a)

(b)

(c)

(d)

Figure 4: Soil temperature field with different cold source temperatures. (a) −5°C. (b) −10°C. (c) −15°C. (d) −20°C.

cold source) was 0.75°C and the final stable temperature of the measuring points nearest to the cold source (0.5 cm away from the cold source) was −3°C.

(6) The lower the cold source temperature was, the faster the soil temperature change rate was and the lower the final stable temperature was. When the temperatures of the cold source were −5°C, −10°C, −15°C, and −20°C, the final stable temperatures of the farthest measuring point (6.75 cm away from the cold source) were 0.75°C, −3°C, −4°C, and −7.5°C, respectively. The temperature differences between the stable temperatures and the corresponding cold sources were 5.75°C, 7°C, 9°C, and 12.5°C, respectively. The lower the cold source temperature was,

the greater the temperature difference was. This showed that the range of frozen soil expansion did not increase linearly with the decrease of the freezing temperature, and there was a limit radius of frozen soil expansion. When the radius was reached, the frozen soil did not expand outward.

In the temporary frozen soil areas, with the seasons and day and night temperature changes, natural frozen soils will produce changes in freeze-thaw cycles. In the process of artificial freezing, due to power failures, freezing pipe fractures, salt water leakages, and other reasons, the freezing process will be interrupted, and the frozen soil will thaw. With measures taken to restore the freezing, the thawed frozen soil will start to freeze again, and the freezing and
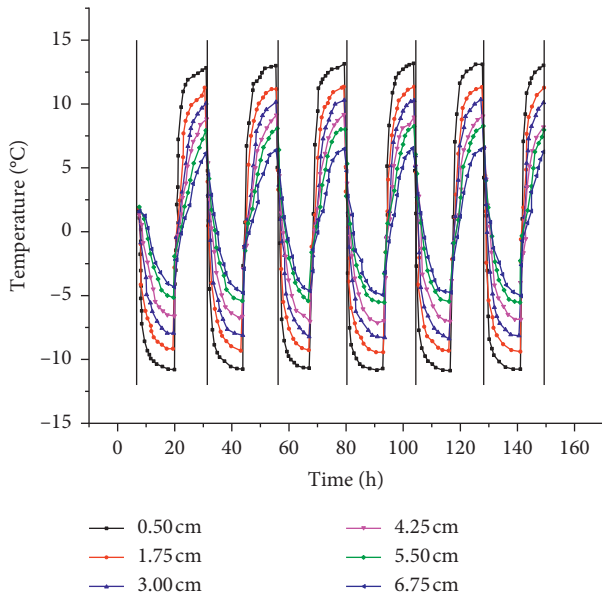
FIGURE 5: Soil temperature field with freeze-thaw cycles.

thawing processes will also occur. In this experiment, the experimental conditions were closed and undrained, and the amount of soil and water in the test tube did not change. Under freeze-thaw cycles conditions, the soil temperature field changed periodically.

3.2.2. Frost Heaving Rate. When the temperature was −15°C, the relationship between the frost heaving rate and time is shown in Figure 6.

It can be seen from Figure 6 that, during the beginning of freezing, the frost heaving rate was reduced and became a negative value; that is, the phenomenon of "freeze shrinkage" occurred. This phenomenon was caused by the negative pore water pressure in the soil during the beginning of freezing, which reduced the volume of the soil. When the volume reduction caused by the negative pore water pressure was greater than the increase caused by water freezing, the total volume of soil decreased. After the freezing shrinkage reached the critical point, the frost heaving began to occur in the soil. The frost heaving continued to increase and finally tended to be stable. The test results of the soil frost heaving rate for different freezing temperatures are shown in Table 2. The values in Table 2 are the frost heave rates at the stable stage of freezing, that is, the maximum frost heaving rates.

The experimental data were plotted on a scatter plot, and it was judged that the frost heaving rate and the freezing temperature were approximately linearly related according to the image. Therefore, linear fitting was performed to obtain the correlation coefficient R Square = 0.98605, which showed a good fitting effect. The results of the fitting test are shown in Figure 7.

Combining Table 2 and Figure 7, it can be seen that, within the range of the test conditions, the frost heaving rate of the soil became larger as the freezing temperature decreases, which was roughly linear.
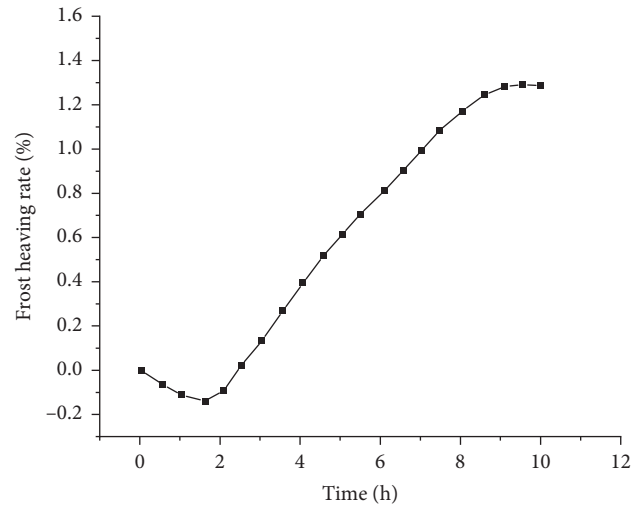

FIGURE 6: The relationship between frost heaving rate and time.

TABLE 2: Frost heaving rate for different freezing temperatures.

Temperature (°C)	−5	−10	−15	−20
Frost heaving rate (%)	0.53	0.78	1.22	1.41

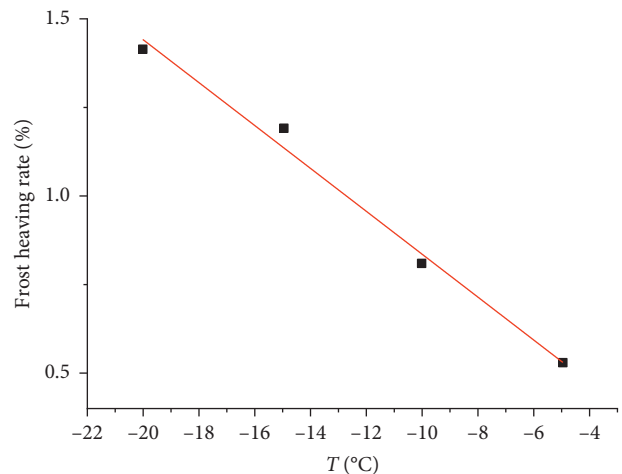| Equation	$y = a + b * x$		
Weight	No weighting		
Residual sum of squares	0.00456		
Pearson's r	−0.99508		
Adj. R^2	0.98529		
		Value	Standard erro
B	Intercept	0.23009	0.05831
	Slope	−0.06055	0.00426

FIGURE 7: The relationship between the frost heaving rate and the freezing temperature.

3.2.3. Frost Heaving Force. When the temperature was −15°C, the relationship between the frost heaving force and time was as shown in Figure 8.

According to Figure 8, the frost heaving force of the soil gradually increased with the freezing time and finally tended
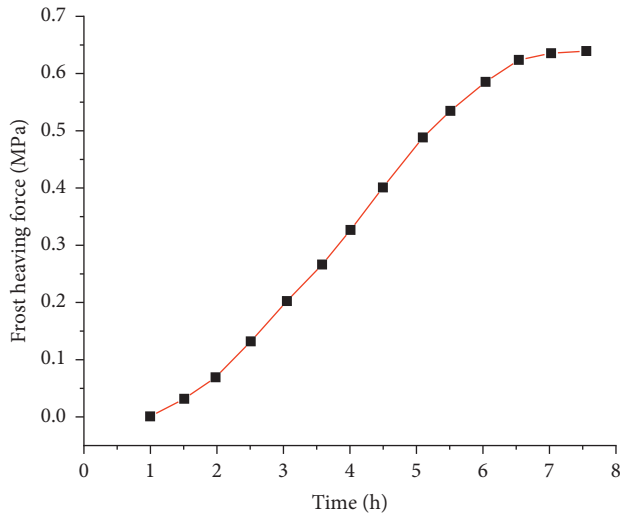
FIGURE 8: The relationship between the frost heaving force and time.

to be flat. Due to the limitation of experimental instruments, only the compressive stress could be detected. That is, the frost heaving force could be monitored at the stage of frost heaving rate increasing. The frost heaving force in the freezing shrinkage stage could not be monitored, and its value was 0 by default. The test results of the soil frost heaving force for different freezing temperatures are shown in Table 3. The values in Table 3 are the frost heave forces at the stable stage of freezing, that is, the maximum frost heaving forces.

The experimental data were plotted on a scatter plot, and it was judged that the frost heaving force and the freezing temperature were approximately linearly related according to the image. Therefore, a linear fitting was performed to obtain the correlation coefficient R Square $= 0.97396$, which showed a good fitting effect. The results of the fitting test are shown in Figure 9.

Combining Table 3 and Figure 9, it can be seen that, within the range of the test conditions, the frost heaving force of the soil increased with the decrease of the freezing temperature, which was roughly linear. In the experiment, the maximum frost heaving rate and the maximum frost heaving force of each layer of soil samples at $-10°C$ were as shown in Table 4.

4. Numerical Simulation Analysis of Thermomechanical Coupling

4.1. Model Parameters. A three-dimensional numerical model was established to simulate the variation law of the formation temperature field and the frost heaving caused by the actual freezing condition. Taking the vertical plane passing through the longitudinal axis of the connecting passage as the symmetry plane, the 1/2 finite element model was established. The material thermal physical parameters of each part are shown in Table 5.

4.2. Model Building. The finite element model was established according to the actual situation of the freezing project. The model of the tunnel and the freezing pipes is

TABLE 3: Values of frost heaving forces at different temperatures.

Temperature (°C)	−5	−10	−15	−20
Frost heaving force (MPa)	0.37	0.46	0.64	0.74

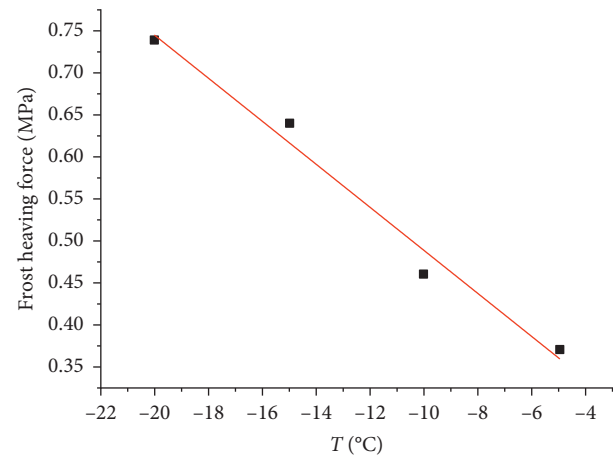| Equation	$y = a + b * x$		
Weight	No weighting		
Residual sum of squares	0.00154		
Pearson's r	−0.99079		
Adj. R^2	0.9725		
		Value	Standard erro
B	Intercept	0.23266	0.03388
	slope	−0.02561	0.00247

FIGURE 9: The relationship between the frost heaving force and the freezing temperature.

TABLE 4: Frost heaving test results.

Layer	Soil properties	Frost heaving rate (%)	Frost heaving force (MPa)
1	Silt	0.92	0.71
2	Clay	0.78	0.46
3	Silty soil	0.76	0.57
4	Muddy sand	0.69	0.15

shown in Figure 10, and the finite element model after meshing is shown in Figure 11.

4.3. Numerical Simulation Analysis of Temperature Field. A transient thermal calculation was carried out for the development of the soil temperature field in the active freezing period. The distribution cloud charts of the soil temperature field were selected when the freezing times were 15 d, 30 d, 45 d, and 60 d, with 15 d as the interval, as shown in Figure 12.

When freezing, the temperature of the soil around the freezing pipes began to drop rapidly, and the frozen soil cylinder was gradually formed around the freezing pipes. With the increase of the freezing time, the frozen soil cylinder developed outward along the radial direction of the

TABLE 5: Material thermal physical parameters.

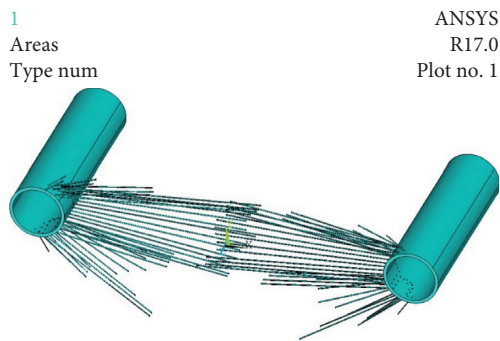| Material	Specific heat capacity C (kJ·kg^{-1}·k^{-1})		Thermal conductivity K (w·m^{-1}·k^{-1})		Enthalpy H (×10^6 J m^{-3})			
	−30∼−3°C	0∼40°C	−30°C	40°C	−30°C	−3°C	0°C	40°C
Miscellaneous fill	1.30	1.50	1.40	1.10	0	63.8	187.8	269.6
Silt	1.70	1.90	1.49	1.31	0	71.6	415.0	504.7
Clay	1.48	1.68	1.67	1.44	0	72.7	294.0	386.1
Silty soil	1.54	1.76	1.82	1.23	0	67.2	389.8	473.6
Muddy sand	1.18	1.52	1.53	1.24	0	91.3	320.2	432.8
Tunnel segment	0.97		1.28		—			

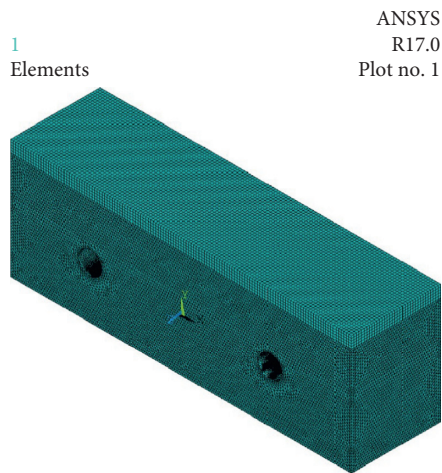FIGURE 10: Freezing pipes and tunnel model.

FIGURE 11: Model meshing.

freezing pipes. After 30 days, most of the adjacent frozen soil had intersected, and areas with the higher temperature gradually decreased with the continuous freezing. When the freezing time reached 60 days, the thickness of the freezing curtain could reach the design requirement of 2.1 m.

4.4. Thermal-Mechanical Coupling Simulation and Analysis. To explore the coupling evolution law of the freezing temperature field and soil displacement field, the thermal-mechanical coupling solution was carried out. The distribution of the soil displacement field under the thermal load is shown in Figure 13.

The frost heaving of the soil around the freezing pipes was caused by freezing, and because of the uneven distribution of the freezing pipes, the overall frost heaving was not uniform. When freezing for 15 days, the larger frost heaving areas were scattered. When freezing for 30 days, the freezing curtain gradually intersected. The frost heaving areas also showed a homogenization phenomenon and gradually gathered and merged. When freezing for 60 days, the frost heaving areas at the top were connected as a whole, showing a phenomenon of the middle parts being large and the two sides being small. Then as the freezing continued, the frost heaving areas were further homogenized and gradually spread from the middle area to both sides, finally becoming steady.

According to the calculation results, the maximum frost heaving of the strata occurred above the middle of the connecting passage. To further analyze the distribution law of the frost heaving at this position, the displacement duration curve of the maximum displacement area was drawn for analysis, as shown in Figure 14. The whole frost heaving process could be roughly divided into two stages. The first was the frost heaving generation stage, during which the frost heaving began to slowly increase. The second stage was the frost heaving development stage, during which the frost heaving began to increase rapidly and reached the maximum value of 193.03 mm in 65 days.

5. Comparative Analysis of Measured Data

5.1. Freezing Temperature Field Measurement. To accurately understand the development law of the freezing curtain in the long connecting passage, temperature measuring points were arranged in the surrounding strata to obtain the temperature field data of the freezing curtain. The layout of the freezing holes and the temperature measuring holes on the left side of the connecting passage are shown in Figure 15.

The temperature measuring points were arranged at 5 m, 12 m, and 19 m of the hole depth to monitor the development of the temperature field at different depth sections. The temperature measuring points were numbered Ti–j, the labels i = 1–8 were used according to the different temperature measuring holes, and the labels j = 1–3 were used according to different positions of 5 m, 12 m, and 19 m along with the hole depth. The temperature measuring hole T5 was located at the edge of the excavation area, and T7 was located
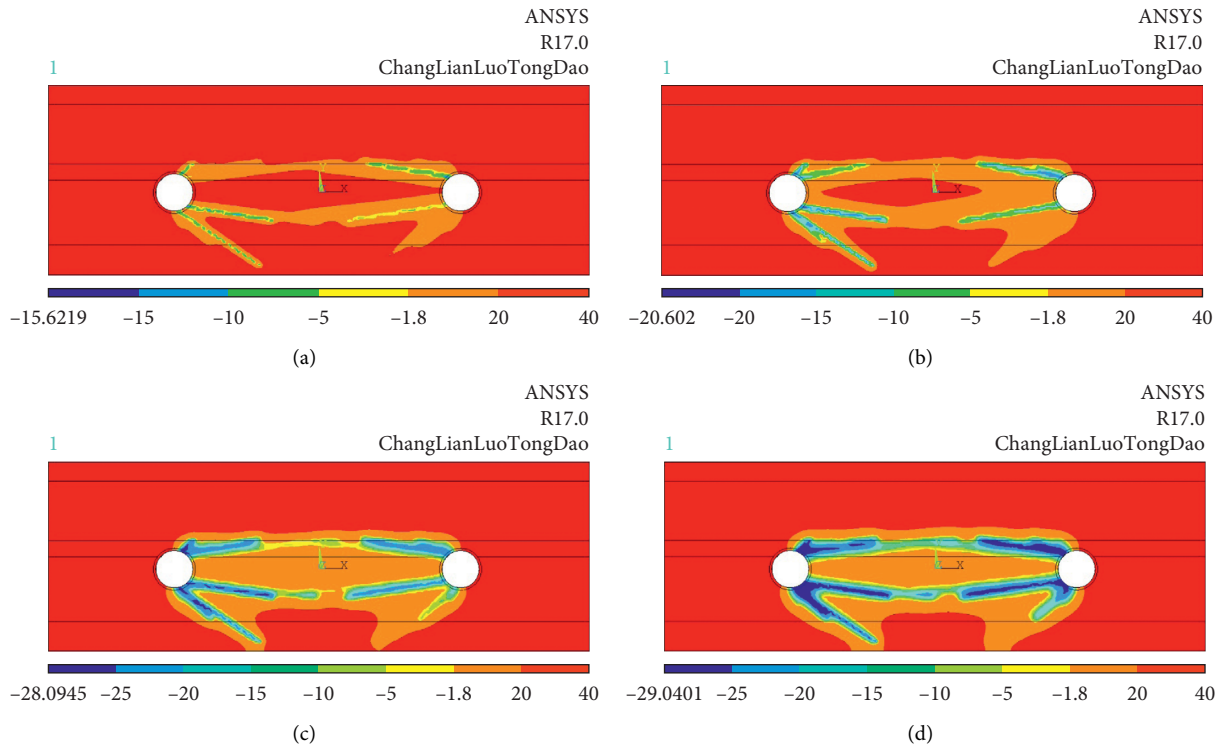
Figure 12: The distribution cloud charts of the freezing temperature fields. (a) 15 d. (b) 30 d. (c) 45 d. (d) 60 d.
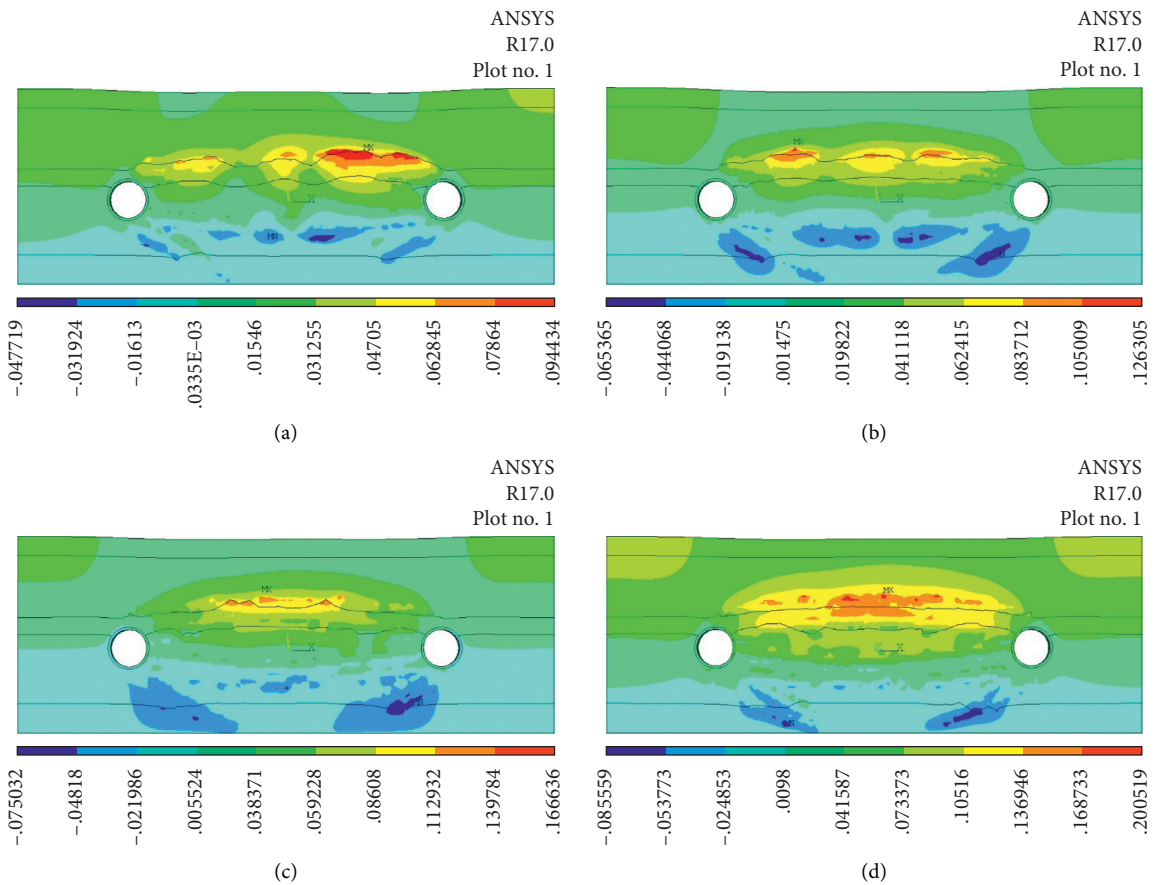

Figure 13: The distribution cloud charts of the displacement field. (a) 15 d. (b) 30 d. (c) 45 d. (d) 60 d.
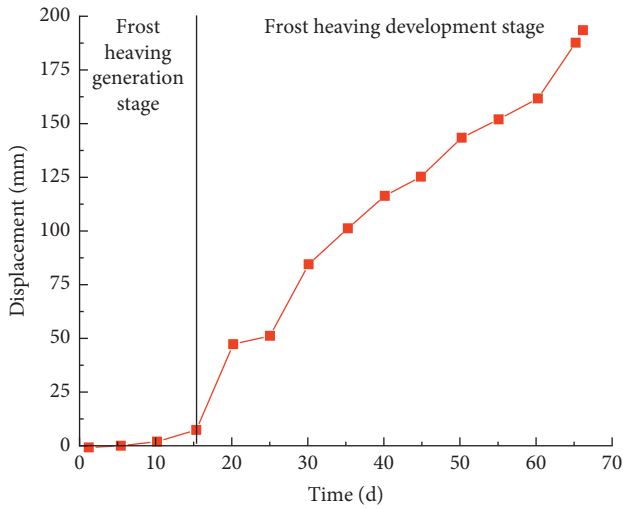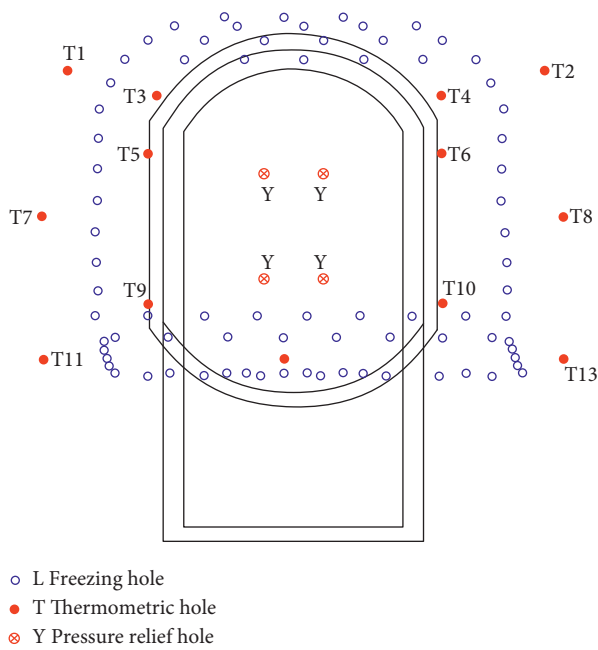
FIGURE 14: The displacement duration curve.

FIGURE 16: Relationship between temperature and time for T5.

- ○ L Freezing hole
- ● T Thermometric hole
- ⊗ Y Pressure relief hole

FIGURE 15: Holes on the left side of the connecting passage.
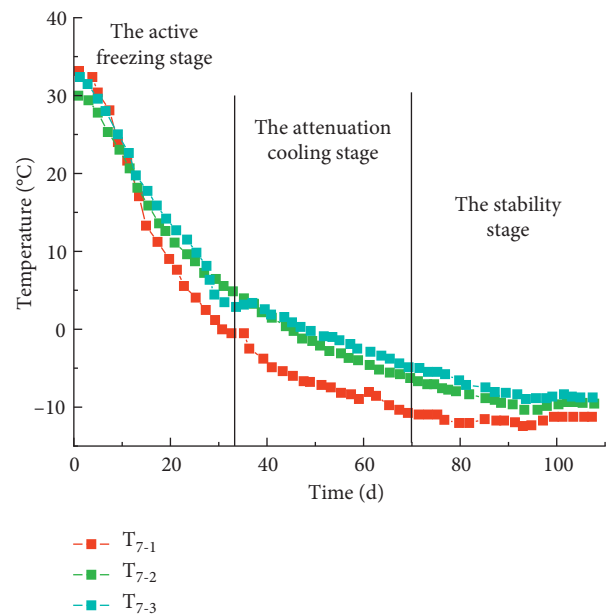
FIGURE 17: Relationship between temperature and time for T7.

at the edge of the nonexcavation area. The temperature and time relationship curves of the measuring points at different depths are shown in Figures 16 and 17.

The temperature trends for T5 and T7 temperature measuring holes were basically the same, and the entire freezing process could be divided into the active freezing stage, the attenuation cooling stage, and the stability stage. In the active freezing stage, the formation temperature decreased rapidly, lasting for about 40 days. In the attenuation cooling stage, the temperature of the formation was close to 0°C, and the moisture in the soil began to solidify into ice. Due to the effect of the latent heat of the phase change, the temperature slowed down. In the stability stage, the formation temperature dropped to a negative temperature, and the latent heat of the phase change was completed. The soil
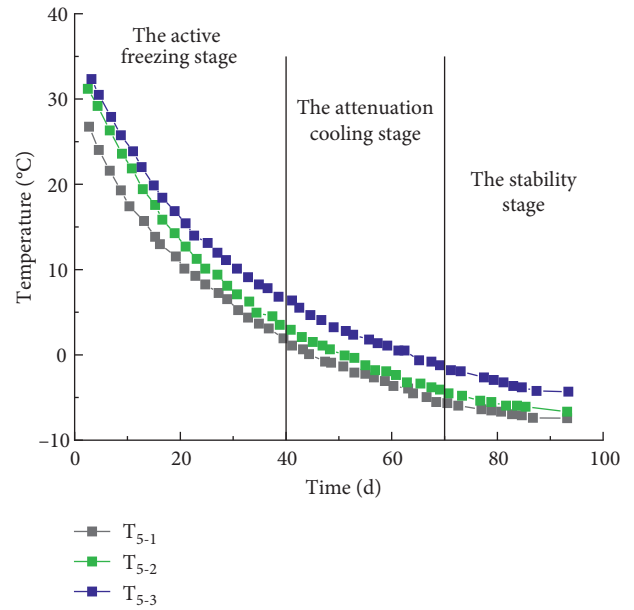
temperature continues to slow down and finally tended to be stable.

The temperature at the T4-3 measuring point was calculated with finite element software and compared with the measured temperature, as shown in Figure 18.

In the early stage of active freezing, there was a certain difference between the simulated temperature and the measured temperature. The temperature drop curve of the finite element simulation was smoother, but the change of the measured temperature drop curve was more violent. During the late stage of the active freezing period and the maintenance freezing period, the simulated temperature and
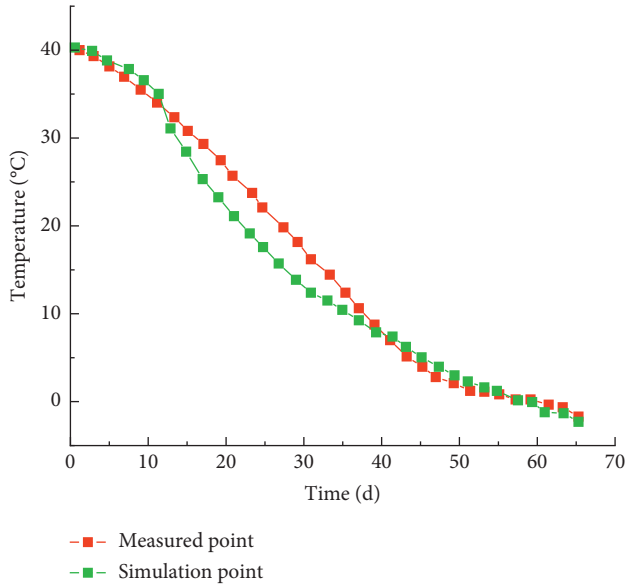
FIGURE 18: Temperature evaluation at temperature measurement point T4−3.

FIGURE 19: Layout of monitoring points.

the measured temperature almost coincided. Therefore, the numerical simulation described above could accurately reflect the variation of the soil temperature field.

5.2. Frost Heaving Measurement.

Forty-one monitoring points were arranged on the ground surface within the freezing influence range of the connecting passage to study the frost heaving law of the freezing project. The layout of the monitoring points is shown in Figure 19.

The measuring points DZ5-1–DZ5-7 were located in the middle of the connecting passage, where the frost heaving was more severe. The measuring points DZ5-1–DZ5-4 were selected as the research object to analyze the distribution law of frost heaving during the freezing period. The distances between DZ5-1–DZ5-7 were 3 m, 5 m, and 7 m, respectively. The measured surface deformation values are shown in Figure 20, and the surface frost heaving duration distribution is shown in Figure 21.

The process of surface uplift caused by frost heaving could be divided into a rapid growth stage and a steady growth stage. The rapid growth stage corresponded to the early and late stages of the active freeze period. The stable growth stage corresponded to the maintenance freeze period, during which the soil temperature was basically stable and the frost heaving was also in a relatively stable state.

The numerical model was used to further study the frost heaving law of frozen soil, and the accuracy of the numerical model was evaluated by comparing the model with the field measured data. The numerical calculation was carried out with the corresponding model position of the DZ5-4 measuring point, and the comparative analysis was carried out with the measured value, as shown in Figure 22.

It can be seen from Figure 22 that there was a small deviation in the middle part, and the initial stage and the final stage were relatively consistent. Generally speaking, the
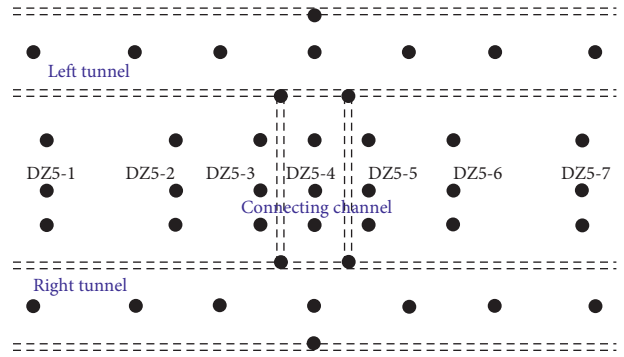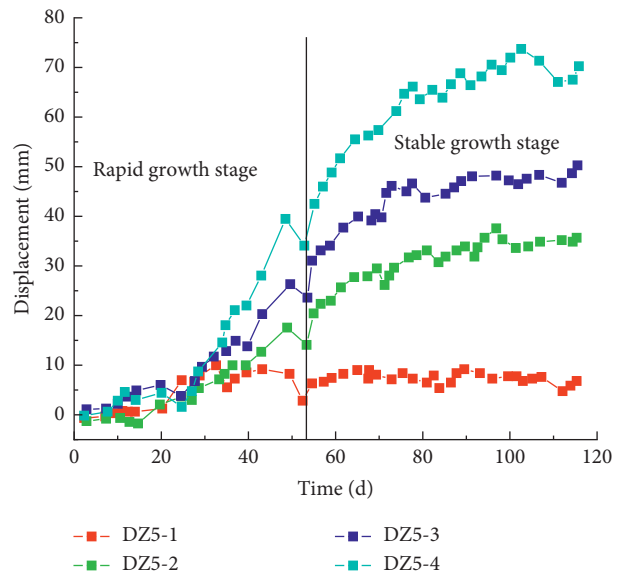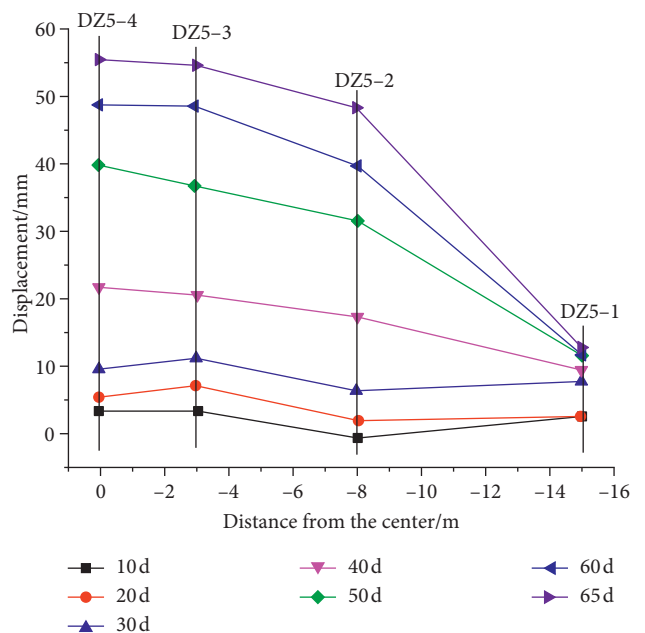

FIGURE 20: Surface deformation value.

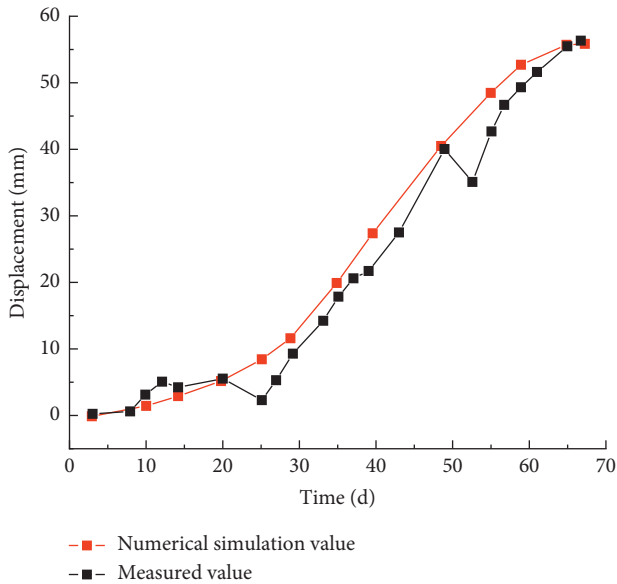FIGURE 21: Distribution of frost heaving duration.

FIGURE 22: Comparison of calculated and measured values.

final calculation results of the numerical simulation were consistent with the measured data. Therefore, the above numerical simulation could accurately reflect the law of soil frost heaving caused by freezing.

6. Conclusions

The temperature field and the frost heaving characteristics are the keys to the study of the freezing method. The temperature field is the most direct inducement for the formation and development of freezing curtain, and frost heaving can cause structural deformation and damage. In this study, the thermal physical parameters and the frost heaving parameters of soil were obtained through the soil thermal physical tests and frozen soil frost heaving tests. A three-dimensional finite element model was established to simulate the temperature field and frost heaving changes of soil under on-site working conditions, and the model was further compared with the field measured values.

(1) Thermal physical tests and frost heaving tests for frozen soil were carried out to study the temperature field, frost heaving rate, and frost heaving force of soil during frost heaving.

(2) The entire cooling process could be roughly divided into three stages: the active freezing stage, the attenuation cooling stage, and the stability stage. The range of frozen soil expansion did not increase linearly with the decrease of the freezing temperature, and there was a limit radius for the frozen soil expansion. When the radius was reached, frozen soil did not expand outward. For the freeze-thaw cycle, the soil temperature changed periodically.

(3) When the freezing temperatures were −5°C, −10°C, −15°C, and −20°C, the frost heaving rates of soil were 0.53%, 0.95%, 1.28%, and 1.41%, and the frost heaving forces of the soil were 0.37 MPa, 0.46 MPa,

0.59 MPa, and 0.74 MPa, respectively. In the range of test conditions, the frost heaving rate and the frost heaving force of the soil increased with the decrease of the freezing temperature, and the relationship was roughly linear with the temperature.

(4) The development of the formation temperature field could be divided into three periods. In the early stage of active freezing, the formation temperature decreased rapidly. In the late stage of active freezing, the temperature dropped slowly. In the maintenance freezing period, the temperature tended to be stable.

(5) In the finite element model, the calculated temperature value corresponding to the T4-3 measuring point was compared with the measured temperature, and the calculated frost heaving value corresponding to the DZ5-4 measuring point was compared with the measured value, which verified the fact that the numerical calculation could reflect the temperature field change and the frost heaving law of the formation accurately.

Data Availability

The figures and tables data used to support the findings of this study are included within the article.

Conflicts of Interest

The authors declare that they have no conflicts of interest.

Acknowledgments

References

[1] G. J. Bouyoucos, "Directions for making mechanical analyses of soils by the hydrometer method," *Soil Science*, vol. 42, no. 3, pp. 225–230, 1936.

[2] D. H. Everett, "The thermodynamics of frost damage to porous solids," *Transactions of the Faraday Society*, vol. 57, pp. 1541–1551, 1961.

[3] R. D. Miller, "The porous phase barrier and crystallization," *Separation Science*, vol. 8, no. 5, pp. 521–535, 1973.

[4] R. R. Gilpin, "A model for the prediction of ice lensing and frost heave in soils," *Water Resources Research*, vol. 16, no. 5, pp. 918–930, 1980.

[5] J. M. Konrad and C. Duquennoi, "A model for water transport and ice lensing in freezing soils," *Water Resources Research*, vol. 29, no. 9, 1993.

[6] Y. Wang, T. Sun, H. Yang, J. Lin, and H. Liu, "Experimental investigation on frost heaving force (FHF) evolution in

preflawed rocks exposed to cyclic freeze-thaw conditions," *Geofluids*, vol. 2021, no. 1, pp. 1–12, 2021.

[7] S. Huang, Y. Ye, and X. Cui, "Theoretical and experimental study of the frost heaving characteristics of the saturated sandstone under low temperature," *Cold Regions Science & Technology*, vol. 174, Article ID 103036, 2020.

[8] L. Huang, Y. Sheng, J. Wu, B. He, X. Huang, and X. Zhang, "Experimental study on frost heaving behavior of soil under different loading paths," *Cold Regions Science and Technology*, vol. 169, pp. 102905–102912, 2020.

[9] P. He, M. Xiong, Y. Mu, J. Dong, and X. Na, "Experimental study on frost-heaving force development of Tibetan clay subjected to one-directional freezing in an open system," *Advances in Civil Engineering*, vol. 2021, no. 5, pp. 1–13, 2021.

[10] F. Yue, P. Chou, and G. Yang, "Design and practice of freezing method applied to connected aisle in tunnel under complex conditio," *Chinese Journal of Geotechnical Engineering*, vol. 28, no. 5, pp. 660–663, 2006.

[11] P. He, G. Chen, and Q. Yu, "A couple model of heat, water and stress fields of saturated soil during freezing," *Journal of Glaciology and Geocryology*, vol. 22, no. 2, pp. 135–138, 2000.

[12] C. Xia, Y. Wang, and i. Zheng, "Study of differential frost heave of fractured rock mass," *Rock and Soil Mechanics*, vol. 41, no. 4, pp. 1161–1168, 2020.

[13] B. Wang, C. Rong, and H. Cheng, "Stress analysis of heterogeneous frozen wall considering interaction with surrounding soil," *Journal of China Coal Society*, vol. 42pp. 354–361, z2, 2017.

[14] K. M. Yoshinaka and Y. Neaupanet, "Simulation of a fully coupled thermo–hydro–mechanical system in freezing and thawing rock," *International Journal of Rock Mechanics and Mining Sciences*, vol. 36, no. 5, pp. 563–580, 1999.

[15] K. M. Neaupane and T. Yamabe, "A fully coupled thermo-hydro-mechanical nonlinear model for a frozen medium," *Computers and Geotechnics*, vol. 28, no. 8, pp. 613–637, 2001.

[16] O. B. Andersland and B. Ladanyi, "Frozen ground engineering," *American Society of Civil Engineers*, vol. 384, 2004.

[17] J. Chen, T. Liu, and D. Li, "Study on artificial three - tube freezing model test and freeze program," *Coal Science and Technology*, vol. 45, no. 12, pp. 94–100, 2017.

[18] Y. Jiang, Y. Zhao, and G. Zhou, "Multi–parameter monitoring of frozen soil structure with super–long freezing hole drilling in Guangzhou metro," *Rock and Soil Mechanics*, vol. 31, no. 1, pp. 158–173, 2010.

[19] W. Qi, P. Yang, and M. Jin, "Application and survey analysis of freezing method applied to ultra–long connected aisle in metro tunnel," *Chinese Journal of Underground Space and Engineering*, vol. 6, no. 5, pp. 1065–1071, 2010.

[20] X. Long, G. Cen, and L. Cai, "Hydro–thermal coupling model test and field validation of uneven frost heave of pavement structure," *Journal of Harbin Institute of Technology*, vol. 51, no. 3, pp. 172–178, 2019.

[21] Y. Zhang, Y. Xie, and Y. Li, "A frost heave model based on space–time distribution of temperature field in cold region tunnels," *Rock and Soil Mechanics*, vol. 39, no. 5, pp. 1625–1632, 2018.

[22] D. Li, A. Lu, and Q. Zhang, "Analysis of freezing method for construction of connected aisle in nanjing metro tunnels," *Chinese Journal of Rock Mechanics and Engineering*, vol. 23, no. 2, p. 334, 2004.

[23] J. Hu and P. Yang, "Numerical analysis of temperature field within large–diameter cup–shaped frozen soil wall," *Rock and Soil Mechanics*, vol. 36, no. 2, pp. 523–531, 2015.

[24] H. Cai, Y. Huang, and T. Pang, "Finite element analysis on 3D freezing temperature field in metro connected aisle construction," *Journal of Railway Science and Engineering*, vol. 12, no. 69, pp. 180–187, 2015.

[25] P. Yang and A. Pi, "Study on the effects of large groundwater flow velocity on the formation of frozen wall," *Chinese Journal of Geotechnical Engineering*, vol. 23, no. 2, pp. 167–171, 2001.

[26] D. Li, R. Wang, and P. Hu, "FEM analysis of transient freezing temperature field of frozen multi–wall tube," *Coal Geology & Exploration*, vol. 2, pp. 38–41, 2007.